Available online at www.sciencedirect.com
SCIENCE DIRECT®
ELSEVIER
Earth and Planetary Science Letters 240 (2005) 621–633
EPSL
www.elsevier.com/locate/epsl

Formation of Paleoproterozoic eclogitic mantle, Slave Province (Canada): Insights from in-situ Hf and U–Pb isotopic analyses of mantle zircons

Stefanie S. Schmidberger [a,*], Larry M. Heaman [a], Antonio Simonetti [a], Robert A. Creaser [a], Harrison O. Cookenboo [b]

[a] *Earth and Atmospheric Sciences, University of Alberta, Edmonton, AB, Canada T6G 2E3*
[b] *Watts, Giffis and McQuat, 620-475 Howe St., Vancouver, BC, Canada V6C 4B3*

Received 18 December 2004; received in revised form 24 September 2005; accepted 25 September 2005
Available online 10 November 2005
Editor: R.D. van der Hilst

Abstract

In-situ Hf isotope analyses and U–Pb dates were obtained by laser ablation-MC-ICP-MS for a zircon-bearing mantle eclogite xenolith from the diamondiferous Jericho kimberlite located within the Archean Slave Province (Nunavut), Canada. The U–Pb zircon results yield a wide range of ages (~2.0 to 0.8 Ga) indicating a complex geological history. Of importance, one zircon yields a U–Pb upper intercept date of 1989 ± 67 Ma, providing a new minimum age constraint for zircon crystallization and eclogite formation. In contrast, Hf isotope systematics for the same zircons display an intriguing uniformity, and corresponding Hf depleted mantle model ages range between 2.1 ± 0.1 and 2.3 ± 0.1 Ga; the youngest Hf model age is within error to the oldest U–Pb date.

The Jericho eclogites have previously been interpreted as representing remnants of metamorphosed oceanic crust, and their formation related to Paleoproterozoic subduction regimes along the western margin of the Archean Slave craton during the Wopmay orogeny. Hf isotope compositions and U–Pb results for the Jericho zircons reported here are in good agreement with a Paleoproterozoic subduction model, suggesting that generation of oceanic crust and eclogite formation occurred between 2.0 and 2.1 Ga. The slightly older Hf depleted mantle model ages (~2.1 to 2.3 Ga) may be reconciled with this model by invoking mixing between 'crustal'-derived Hf from sediments and more radiogenic Hf associated with the oceanic crust during the ~2 Ga subduction event. This results in intermediate Hf isotope compositions for the Jericho zircons that yield 'fictitiously' older Hf model ages.

Keywords: Eclogite; Zircon; Subduction; Archean slave craton; Hf isotopes; Laser ablation-MC-ICP-MS

1. Introduction

Continental mantle roots are composed of cold, refractory peridotites and contribute to the relative stability of Archean cratons. These roots retain a record of their geological history over billions of years (e.g. [1]). Subcratonic lithosphere also contains a small but petrologically significant amount of eclogite, a common upper mantle xenolith in kimberlites [2]. Of great economic interest, mantle eclogites are an important source of diamond in which eclogitic diamond populations dominate a number of world-class deposits (e.g. [3,4]). Contrasting hypotheses have been proposed to

* Corresponding author. Tel.: +1 780 492 0356; fax: +1 780 492 2030.
E-mail address: stefanie.schmidberger@ualberta.ca (S.S. Schmidberger).

0012-821X/$ - see front matter © 2005 Elsevier B.V. All rights reserved.
doi:10.1016/j.epsl.2005.09.057

explain the origin of eclogites; these include magmatic processes at high pressures in the Earth's mantle (e.g. [5]), subduction and metamorphism of altered oceanic crust (e.g. [6]), or subduction of low-pressure cumulates such as gabbros (e.g. [7]). Determining the age of eclogite formation, however, has been proven difficult because of element diffusion and isotope exchange that occurs in many mineral phases at lithospheric temperatures and pressures (e.g. [8,9]). Moreover, mantle xenoliths are typically subjected to repeated episodes of metasomatism including interaction with the host kimberlite magma during sample transport; processes that perturb most radiogenic geochronometers (e.g. Sm–Nd, Rb–Sr; [10,11]). In contrast, Schmidberger et al. [12] clearly demonstrated the relatively robust nature of the Lu–Hf chronometer in resisting significant chemical changes imposed on mantle peridotites by metasomatic activity.

In some mantle-derived xenoliths entrained in kimberlite, including eclogite, zircon is an accessory mineral [13,14]; mantle zircon megacrysts also occur as a rare component in kimberlites (e.g. [15–17]). Previous Hf isotopic and U–Pb studies have reported a variety of genetic models for these megacrysts including formation as metasomatic phases in the subcontinental lithosphere related to kimberlite magmatism [16], origin from ancient subducted oceanic crust [15], or derivation from asthenospheric melts that interacted with subcontinental lithosphere [17]. Moreover, the robustness of zircon is pivotal in deciphering the age of geologically complex samples subjected to eclogite-facies metamorphism (e.g. [18,19]), mainly because of its relative insolubility in most magmas and fluids, high closure temperature to diffusion of elements and resistance to chemical and physical breakdown [20]. To our knowledge, combined Hf isotopic and U–Pb data for 'primary' zircon occurring within mantle xenoliths, however, are sparse. In this paper we present in-situ Hf isotope and U–Pb data for zircons from a single eclogite xenolith obtained by laser ablation-multicollector inductively coupled plasma mass spectrometry (MC-ICP-MS) in order to unravel the origin and age of this sample of mantle eclogite. The results presented here provide important information on the orogenic development of the Archean Slave craton, which includes additional evidence for the occurrence of subduction during the early Proterozoic.

2. Geology and samples

The Slave craton forms part of the Archean Canadian shield and is composed of 4.05 to 3.00 Ga basement gneisses exposed in the central and western portions but is dominated by 2.73 to 2.58 Ga supracrustal assemblages and plutonic suites (e.g. [21,22]). The Slave craton is bounded by the Paleoproterozoic (1.9–1.8 Ga) Wopmay orogen to the west and the 2.0–1.9 Ga Taltson–Thelon orogen to the east and southeast (e.g. [23]). The diamondiferous Jericho kimberlite (Nunavut, Canada; Fig. 1) is located ~400 km northeast of Yellowknife, and intruded the Archean Contwoyto granitic batholith in the western Slave Province 173 Ma ago [14,24,25]. Of interest, the kimberlite was emplaced ~200 km east of the Great Bear magmatic zone, which has been interpreted as a continental magmatic arc that developed ~1.9 Ga ago as the result of east-dipping subduction at the western margin of the Slave craton (e.g. [23,26]; Fig. 1). The mantle xenolith population hosted by the Jericho kimberlite contains a relatively large proportion of eclogites (25%; [27]). The majority of these eclogites have been interpreted as representing remnants of metamorphosed subducted oceanic crust as evidences by their mineral compositions such as trends to high Al, Fe, Na contents in clinopyroxene [27,28]. A number of the Jericho eclogites (2–3%) contain rare accessory zircon [14,27]. These eclogites are characterized by coarse-grained bimineralic compositions consisting of Cr-poor garnet and omphacitic clinopyroxene, and also contain other accessory phases such as rutile and apatite [14]. Zircon mostly occurs as inclusions in constituent garnet and is less common in grain boundaries (Fig. 2). This textural relationship provides evidence that zircon crystallized as part of the original mineral assemblage, and was not introduced during mantle metasomatism that affected the eclogite after its formation. The eclogite whole rocks are extremely enriched in the high field strength elements (HFSE) such as Zr, Hf, Nb, Ta when compared to other eclogites and oceanic mafic rocks (~10–100 times; [14]). Rare earth element patterns show slightly positive Eu anomalies, which is consistent with interpretations that these eclogites are remnants of metamorphosed oceanic crust [14]. Previous U–Pb results obtained by thermal ionization mass spectrometry (ID-TIMS) on zircons from one Jericho eclogite (MX8A) yield highly discordant dates that define a bimodal distribution with upper intercept ages at 1676 Ma and 1061 Ma [14]. The temperature estimate of last equilibration in the lithosphere for eclogite MX8A is ~980 °C [29], when calculated at a nominal pressure of 40 kb corresponding to a depth of ~135 km. Garnet compositions for eclogite MX8A overlap

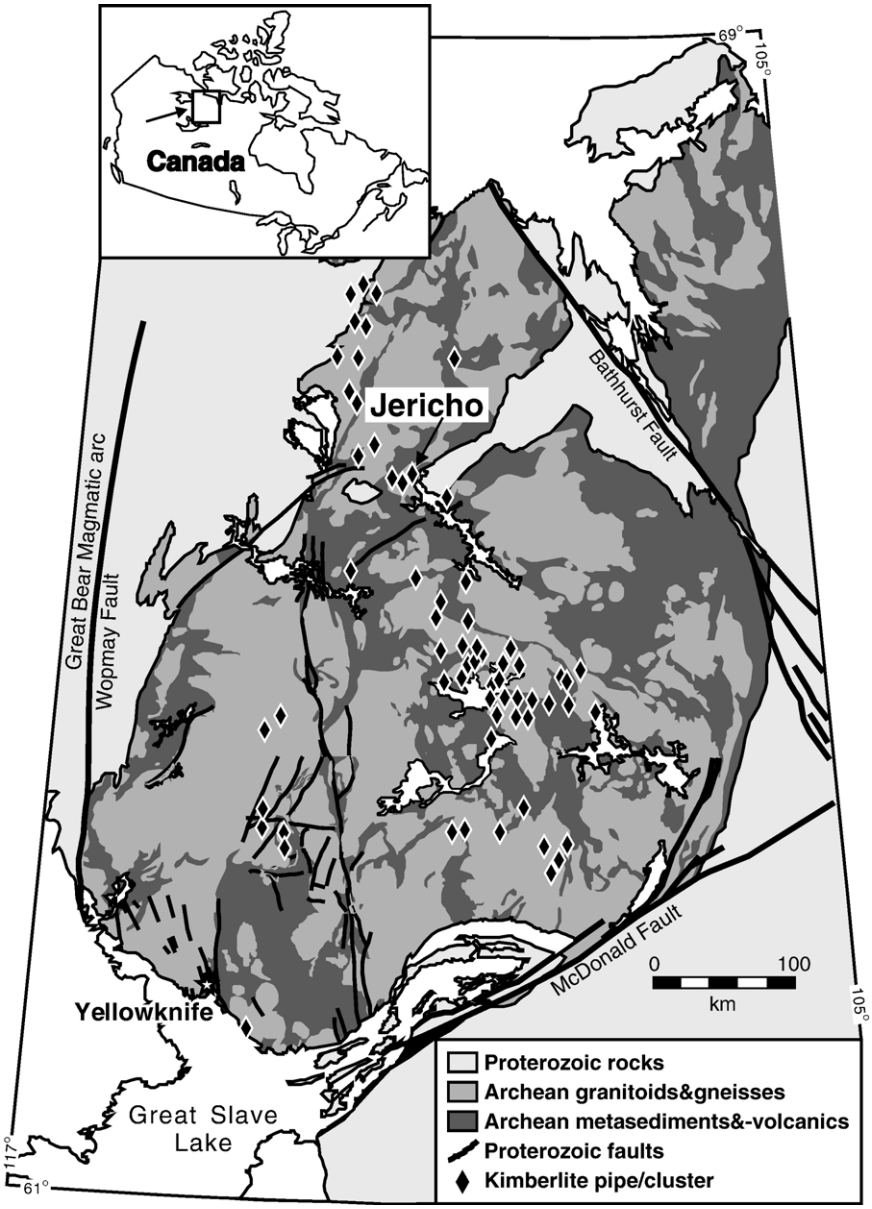

Fig. 1. Geological map of the Slave Province showing kimberlite locations.

the compositional range for garnets from additional Jericho eclogites that have been interpreted as representing subducted oceanic crust ([27]; Fig. 3).

3. Analytical methods

Jericho eclogite MX8A contains abundant large (up to 2 mm) zircon crystals that are colorless and of equant to prismatic habit. Inclusion-free zircon grains from this sample were hand-picked for laser ablation analyses at the University of Alberta Radiogenic Isotope Facility. The zircons were subsequently embedded into epoxy mounts and surfaces polished to 0.3 micron. Laser ablation analyses were obtained using a Nd:YAG UP213 nm laser system (New Wave Research) coupled to a NuPlasma MC-ICP-MS. This instrument is equipped with a modified collector block consisting of 12 Faraday buckets and three ion-counting channels dispersed on the low mass side of the collector array. The collector configuration allows for the simultaneous acquisition of ion signals ranging in mass from ^{238}U to ^{203}Tl, an important factor in obtaining highly precise

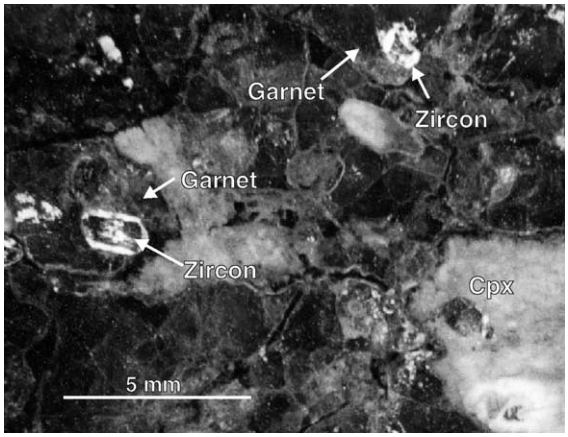

Fig. 2. Photograph of Jericho eclogite MX8A showing textural relationship between constituent eclogite minerals and zircon.

and accurate U–Pb age determinations. ^{207}Pb, ^{206}Pb, and ^{204}Pb (+^{204}Hg) signals are measured on the ion counting channels, whereas U and Tl isotopes are measured on Faraday collectors. Details regarding the analytical protocol employed here for the U–Pb laser ablation analyses are described in Simonetti et al. [30]. Faraday-ion counter bias was determined at the start of each analytical session using a mixed 0.4 ppb standard solution of Pb (NIST SRM 981) and Tl (NIST SRM 997). This approach is similar to that adopted in previous isotopic studies involving MC-ICP- MS instruments equipped with multiple ion-counting devices (e.g. [31]). A routine laser ablation analysis consists of a 30 s blank measurement prior to the start of ablation, which includes correction for the ^{204}Hg contribution (typically ~700 to 1000 cps) measured on a multiplier. Zircons were ablated (30 s ablation time; 160 μm spot size; ~30–40 μm depth; 5 Hz repetition rate; ~7 J/cm^2 energy density) in a He atmosphere (flow rate = 1.00 L/min), and the ablated particles and He gas were simultaneously mixed with a 1 ppb Tl isotopic standard (NIST SRM 997); the latter was aspirated with Ar using a DSN-100 (desolvating nebulizing system) in order to monitor instrumental mass bias. Correction for instrumental drift was achieved by a "standard-sample-standard" bracketing technique involving analysis of the previously dated (ID-TIMS) Mudtank carbonatite zircon for every 10 to 12 Jericho zircons (ablated using identical instrument parameters). The Mud Tank zircon is 732 ± 5 Ma old [32] and contains a Pb concentration (~2 ppm) similar to that found in the eclogitic zircons. The external reproducibility (2σ level) for the analytical protocol was evaluated by repeated analysis of the international SRM NIST 612 glass wafer. During a typical analytical session, the ^{206}Pb/^{238}U and ^{207}Pb/^{206}Pb values reproduced to ≤3% and <1%, respectively [30].

In-situ Hf isotopic measurements were obtained using an analytical protocol similar to that outlined in Machado and Simonetti [33]. Ablations for Hf isotopic analyses (60 s ablation time; 80 μm spot size; ~30–40 μm depth; 5 Hz repetition rate; ~9 J/cm^2 energy density) were placed directly over the spots used for the U–Pb analysis. The external reproducibility for the analytical protocol was evaluated by repeated analysis of the international SHRIMP zircon standard BR266 during the course of this study yielding an average ^{176}Hf/^{177}Hf value of 0.281625 ± 0.000056 (n = 25; 2σ). These values are in excellent agreement with the recently published ^{176}Hf/^{177}Hf value of 0.281621 ± 0.000024 (n = 95; 2σ) for BR266 [34].

The whole rock Jericho eclogite MX8A was crushed and rock chips free of alteration rims were ground in an agate mill. Chemical separation of Hf and Lu for the whole rock eclogite is described in Bizzarro et al. [35]; protocol for solution mode MC-ICP-MS analysis is outlined in Schmidberger et al. [12]. Repeated measurements (n = 18) of a 50 ppb solution of the JMC 475 Hf isotopic standard yield the following average values (and 2σ standard deviation): ^{176}Hf/^{177}Hf = 0.282157 ± 14, ^{178}Hf/^{177}Hf = 1.46728 ± 7, ^{180}Hf/^{177}Hf = 1.88678 ± 25.

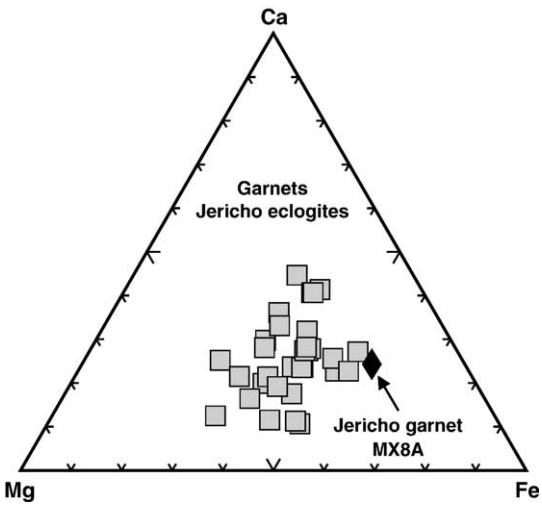

Fig. 3. Molar Mg–Ca–Fe in garnet from Jericho eclogite MX8A. Data for garnet from other Jericho eclogites that have been interpreted as remnants of metamorphosed oceanic crust are shown for comparison [27].

4. Results

In-situ Hf isotope and U–Pb analyses were obtained on all the available 28 zircons crystals that were separated from eclogite sample MX8A. Ablation pits were placed in the core of each grain (Fig. 4) to avoid isotopic differences if present at the crystal margins (thin rims have been reported for some MX8A grains; [14]). Laser ablation U–Pb results are plotted in a concordia diagram (Table 1; Fig. 5), showing that five zircon analyses yield concordant dates and define three age groupings at ~1600 Ma, 1300–1200 Ma and 1100–1000 Ma. U–Pb results for the remaining discordant zircons yield a similar range of upper intercept dates at ~1600 Ma, ~1300 Ma and ~1000 Ma, when regressed through a lower intercept representing the emplacement age (173 Ma) of the Jericho kimberlite (Table 1). The error ellipses associated with the laser ablation-MC-ICP-MS results are much larger than for ID-TIMS analysis; the former are mainly due to the low concentrations of Pb (0.7–3.4 ppm; [14]) present in these Jericho zircons. U–Pb dating of such low Pb abundance zircons using MC-ICP-MS instruments containing an all Faraday collector array would prove extremely difficult or virtually impossible. A typical laser ablation analysis using the multiple ion counter configuration employed here consumes a much lower sample volume (and corresponding total amount of Pb) compared to other ICP-MS instrument configurations and ID-TIMS analyses (sample volume is several orders of magnitude higher; discussed in [30]). The high spatial resolution and low sample volume consumption features associated with the laser ablation analyses reported here are important capabilities when investigating complexly chemically zoned zircons, such as those from Jericho [14]. The typical uncertainty (2σ level) associated with the $^{207}Pb/^{206}Pb$ measurement for an individual laser ablation analysis is <1%. In comparison, ID-TIMS analyses typically report much lower uncertainties in order of ~0.01% associated with the $^{207}Pb/^{206}Pb$ measurement. An additional advantage of the laser ablation-MC-ICP-MS protocol over ID-TIMS is its more rapid nature (i.e. 30 s analysis time compared to 2 or more hours), thus permitting a greater number of analyses in the same period of time. Thus, the most important implications to draw from the laser ablation-MC-ICP-MS U–Pb results presented here (Table 1; Fig. 5) are their similar patterns of discordance and upper intercept ages as those obtained by ID-TIMS analyses.

Fig. 4. Microphotograph of laser ablation pit within zircon crystal from Jericho eclogite.

Most importantly, one zircon grain defines a Paleoproterozoic upper intercept date of 1989 ± 67 Ma (grain Z-4; Table 1) when anchored at 173 Ma (Fig. 5A); and hence places a new minimum age constraint on primary zircon growth and eclogite formation. This date is significantly older than the 1676 Ma upper intercept age obtained by U–Pb ID-TIMS zircon analysis for the same sample [14], which could reflect the fact that a larger zircon population was investigated by laser ablation-MC-ICP-MS analysis compared to that used for ID-TIMS analysis ($n = 28$ versus $n = 6$, respectively). Three zircon grains yield older upper intercept ages (2055 to 2300 Ma), however, these analyses are highly discordant (85–90%) and plot very close to the 173 Ma age of kimberlite emplacement (Table 1). These highly discordant U–Pb results do not provide very reliable upper intercept age information and are thus not used to constrain the age of zircon formation. Most importantly, however, the in-situ results presented here reflect the advantage of high spatial resolution (i.e. concentrating on the cores of structured grains) of in-situ analysis by laser ablation-MC-ICP- MS.

In-situ Hf isotope data were obtained on the same individual zircons and yield a restricted range of $^{176}Hf/^{177}Hf$ values from 0.28152 ± 2 to 0.28169 ± 2 (Table 2; Fig. 6) at the time of kimberlite emplacement (173 Ma ago). The $^{175}Lu/^{176}$ Hf ratios and $^{173}Yb/^{177}Hf$ ratios are very low and range from 0.00003 to 0.00017 and 0.0017 to 0.0082, respectively (Table 2). Due to the extremely low $^{175}Lu/^{176}Hf$ ratios in the zircons, initial $^{176}Hf/^{177}Hf$ ratios are almost identical to those at the time of kimberlite emplacement and the correction for radiogenic decay is smaller than the internal precision for individual analyses. The Hf model ages (T_{DM}) for individual zircons range from 2.1 ± 0.1 to 2.3 ± 0.1 Ga (errors calculated using 2σ external reproducibility), when calculated for derivation from a depleted mantle reservoir (present day

Table 1
U–Pb results for zircon in eclogite MX8A

Grain #	$^{206}Pb/^{204}Pb$	$^{206}Pb/^{238}U$	$^{207}Pb/^{235}U$	$^{207}Pb^*/^{206}Pb^*$	Upper intercept age[a] (Ma)	$^{206}Pb/^{238}U$ Age (Ma)	$^{207}Pb/^{235}U$ Age (Ma)	Disc. %
Z-1	Infinite	0.0409 ± 2	0.3545 ± 11	0.0628 ± 3	1298 ± 89	259 ± 1	308 ± 1	80
Z-2	Infinite	0.2011 ± 19	2.7072 ± 23	0.0968 ± 8	1621 ± 41	1181 ± 10	1330 ± 1	27
Z-3	8264	0.2322 ± 12	2.7003 ± 16	0.0844 ± 2	1296 ± 25	1346 ± 7	1328 ± 1	
Z-4	Infinite	0.2445 ± 40	4.026 ± 22	0.0920 ± 15	1989 ± 67	1410 ± 21	1639 ± 5	29
Z-5	Infinite	0.1672 ± 10	1.6915 ± 14	0.0734 ± 1	1028 ± 26	997 ± 5	1005 ± 1	
Z-6	Infinite	0.0394 ± 3	0.3460 ± 11	0.0635 ± 4	1421 ± 120	249 ± 2	302 ± 1	82
Z-7	9358	0.0400 ± 3	0.3963 ± 11	0.0718 ± 3	1853 ± 100	253 ± 2	339 ± 1	86
Z-8	1170	0.0800 ± 12	0.6973 ± 16	0.0632 ± 2	806 ± 48	497 ± 7	537 ± 1	38
Z-9	2674	0.0495 ± 11	0.5041 ± 17	0.0738 ± 8	1590 ± 130	312 ± 6	415 ± 1	80
Z-10	1568	0.1041 ± 20	0.9904 ± 23	0.0689 ± 7	972 ± 68	638 ± 12	699 ± 1	34
Z-11	Infinite	0.1117 ± 60	1.4294 ± 61	0.0938 ± 4	1650 ± 260	682 ± 35	901 ± 3	59
Z-12	Infinite	0.0380 ± 6	0.3967 ± 16	0.0740 ± 11	2164 ± 210	241 ± 3	339 ± 1	89
Z-13	2569	0.0453 ± 12	0.4106 ± 17	0.0652 ± 6	1322 ± 270	285 ± 8	349 ± 1	78
Z-14	1420	0.0360 ± 1	0.3291 ± 11	0.0664 ± 3	1846 ± 130	228 ± 1	289 ± 1	88
Z-15	1043	0.0880 ± 10	1.0697 ± 15	0.0881 ± 6	1626 ± 50	544 ± 6	739 ± 1	67
Z-16	2164	0.0338 ± 1	0.2959 ± 11	0.0635 ± 4	1876 ± 180	214 ± 1	263 ± 1	89
Z-17	infinite	0.2818 ± 14	3.5459 ± 18	0.0913 ± 2	1440 ± 23	1601 ± 7	1537 ± 1	
Z-18	infinite	0.0890 ± 18	1.0209 ± 21	0.0828 ± 5	1487 ± 110	549 ± 11	714 ± 1	63
Z-19	infinite	0.0334 ± 4	0.2833 ± 11	0.0615 ± 3	1761 ± 220	212 ± 2	253 ± 1	88
Z-20	1855	0.2200 ± 59	2.4064 ± 60	0.0781 ± 7	1169 ± 120	1282 ± 31	1244 ± 2	
Z-21	infinite	0.0567 ± 8	0.5692 ± 15	0.0733 ± 8	1408 ± 97	356 ± 5	458 ± 1	75
Z-22	infinite	0.2701 ± 57	3.7201 ± 58	0.0998 ± 4	1628 ± 87	1541 ± 29	1576 ± 1	
Z-23	infinite	0.0847 ± 15	0.8417 ± 18	0.0721 ± 4	1149 ± 100	524 ± 9	620 ± 1	54
Z-24	infinite	0.0479 ± 10	0.5678 ± 17	0.0855 ± 9	2055 ± 130	302 ± 6	456 ± 1	85
Z-25	infinite	0.0353 ± 4	0.3563 ± 12	0.0731 ± 5	2300 ± 190	224 ± 2	309 ± 1	90
Z-26	infinite	0.1494 ± 31	1.7576 ± 33	0.0853 ± 2	1390 ± 97	898 ± 16	1030 ± 1	35
Z-27	3061	0.1687 ± 13	1.7588 ± 17	0.0756 ± 2	1096 ± 27	1005 ± 7	1030 ± 1	8
Z-28	10833	0.1358 ± 8	1.3154 ± 13	0.0701 ± 2	958 ± 30	821 ± 5	852 ± 1	14

[a] Upper intercept ages are regressed through a lower intercept representing the emplacement age (173 Ma) of the Jericho kimberlite. All errors are 1 sigma uncertainties.

$^{176}Hf/^{177}Hf$ value of 0.2832, ε_{Hf} value of +15; [36] and references therein; Fig. 6). This corresponds to initial ε_{Hf} values of +7.8 to +8.5. The eclogite whole rock MX8A is characterized by a T_{DM} age of 2.2 Ga (Table 2) corresponding to an initial ε_{Hf} value of +8.0, which plots within the range defined by individual zircon analyses (Fig. 6). The match between whole rock and zircon in-situ Hf isotope composition is a compelling result since the former was determined using ion exchange chromatography combined with solution mode MC-ICP-MS analysis; thus providing independent evidence supporting the zircon Hf isotope laser ablation results.

5. Discussion

5.1. Timing of eclogite formation

The uniformity of the zircon Hf isotope results is intriguing and indicates that all zircons in eclogite MX8A share a common origin and formational history. Hf model ages calculated for derivation from a melt-depleted mantle reservoir, a source region commonly proposed for most oceanic crust, suggest that the Jericho zircons crystallized in the Paleoproterozoic. Although episodic zircon growth over millions of years cannot be ruled out, it appears highly unlikely that zircons formed by different mantle-derived melts or fluids over time would be characterized by such uniform Hf isotope compositions. The Hf isotope data impose important constraints for the interpretations of the zircon U–Pb results, since variable U–Pb ages may be the result of ancient Pb loss or multiple periods of zircon growth [37]. The range in concordant U–Pb ages cannot be interpreted as recording multiple episodes of new zircon formation, since this interpretation would be at odds with their uniform Hf isotopic compositions. Thus, the U–Pb zircon chronometer did not remain completely closed to isotope exchange in most grains. However, the Paleoproterozoic upper intercept age of 1989 ± 67 Ma for one Jericho zircon from sample MX8A

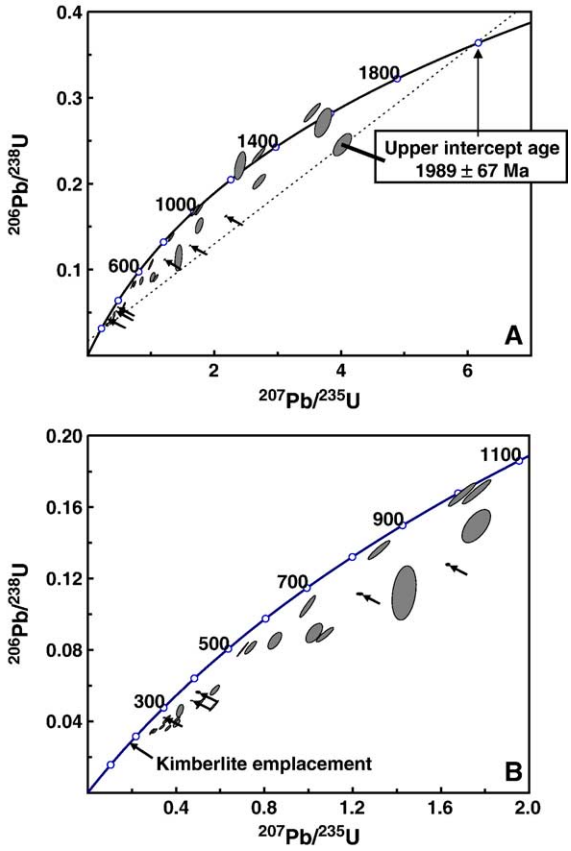

Fig. 5. U–Pb concordia diagram for zircon analyses from Jericho eclogite MX8A obtained by laser ablation-MC-ICP-MS (grey ellipses); (A) oldest upper intercept date is 1989 Ma, (B) many discordant analyses plot close to lower intercept representing kimberlite emplacement age. Also shown are ID-TIMS zircon data (black ellipses identified with arrows; [14]). Error ellipses are 2σ; age labels on concordia curve in Ma.

(grain Z-4; Table 1) provides a new minimum age constraint for eclogite formation.

There is an excellent positive correlation between upper intercept ages and corresponding grain size for individual zircon analyses; i.e. larger grains indicate older upper intercept ages (Fig. 7). This correlation suggests that the Jericho zircons experienced loss of radiogenic Pb as the result of element diffusion. Experimental studies on cation diffusion rates demonstrate that although closure temperatures for Pb mobility in zircon are relatively high (>900 °C; [38]), these are similar to temperature estimates of last equilibration in the mantle for eclogite MX8A (~980 °C at 40 kb). Closure temperatures for the diffusion of U and Th in zircon are higher than that of Pb (1167 °C and 1193 °C, respectively; [20]). The closure of the U-(Th)-Pb system to isotope exchange in Jericho zircon is thus entirely controlled by the diffusion of Pb [20,38]. Experimentally determined diffusion data for natural zircon [38] indicate that at 1000 °C (this approximates the temperature of last equilibration of eclogite MX8A at ~980 °C) complete Pb loss would occur over a time period of 20 to 30 Ma. Thus, based on the results listed in Table 1 and shown in Fig. 5, Pb loss experienced by the Jericho zircons could not have been continuous from the time of eclogite formation to ~800 Ma (the youngest recorded age); the Pb loss was most probably episodic and over time intervals on the order of millions of years. Alternatively, the temperature of last equilibration estimated for eclogite MX8A based on its mineral compositions is too high and the result of a thermal perturbation associated with the kimberlite emplacement. It is therefore possible that the Jericho zircons have resided at somewhat lower temperatures and could have been subjected to continuous Pb loss over time as the result of slow lithospheric cooling. Zircons yielding concordant U–Pb dates have also experienced episodic loss of radiogenic Pb and plot on ancient paleo-diffusion curves, i.e. trajectories that define lines on a concordia diagram with maximum curvature close to the lower intercept age (e.g. [39,40]). Their "dates" record the time when the closure temperature was last attained in individual crystals (i.e. at ~1600 Ma, 1300–1200 Ma and 1100–1000 Ma; Fig. 5A), most probably following cooling after short-term thermal events rather than slow cooling of the lithosphere. Known thermal events that could have affected the lithospheric mantle beneath the Slave craton in the Proterozoic include the Malley (~2230 Ma; [41]), Lac de Gras (~2030 Ma; [41]), Mackenzie (~1270 Ma; [42]), Gunbarrel (~780 Ma; [43]) or the Franklin igneous events (~720 Ma; [44]).

The highly discordant analyses plot very close to the lower intercept coinciding with the emplacement age of the host kimberlite (Fig. 5B), indicating that significant Pb-loss occurred in these zircons up to the time of kimberlite magmatism. The thermal perturbation probably occurred just prior to or during sample entrainment over a limited period of time since the zircons that yield concordant analyses essentially remained closed to Pb diffusion during this event.

Experimental studies on cation diffusion rates indicate that Hf is characterized by very low diffusion rates in zircon and a closure temperature of 1079 °C, which is significantly higher than that for Pb [20]. Therefore, Hf in zircon is essentially immobile at temperature conditions of last equilibration estimated for eclogite MX8A. The uniformity of the laser ablation Hf isotope results obtained here (Table 2) concur with the experi-

Table 2
Hf isotope data for zircon in eclogite MX8A

Grain #	$^{176}Hf/^{177}Hf$	$^{176}Hf/^{177}Hf$ (at 173 Ma)	T_{DM} (Ga)	$^{176}Hf/^{177}Hf$ (at T_{DM})	ε_{Hf} (at T_{DM})	$^{176}Lu/^{177}Hf$	$^{173}Yb/^{177}Hf$	$^{178}Hf/^{177}Hf$	Total Hf Int (V)
Z-1	0.28157 ± 2	0.28157	2.3	0.28156	8.0	0.00010	0.00499	1.46745 ± 10	3.83
Z-2	0.28155 ± 2	0.28155	2.3	0.28154	7.9	0.00012	0.00613	1.46722 ± 12	3.81
Z-3	0.28157 ± 1	0.28157	2.3	0.28157	8.0	0.00012	0.00625	1.46763 ± 16	4.33
Z-4	0.28165 ± 1	0.28165	2.2	0.28164	8.3	0.00003	0.00174	1.46728 ± 13	5.22
Z-5	0.28159 ± 2	0.28159	2.2	0.28159	8.1	0.00009	0.00482	1.46736 ± 15	3.93
Z-6	0.28160 ± 2	0.28160	2.2	0.28160	8.1	0.00010	0.00536	1.46730 ± 12	4.38
Z-7	0.28161 ± 2	0.28161	2.2	0.28161	8.2	0.00005	0.00259	1.46733 ± 12	3.73
Z-8	0.28152 ± 2	0.28152	2.3	0.28152	7.8	0.00012	0.00625	1.46748 ± 13	4.08
Z-9	0.28158 ± 1	0.28158	2.2	0.28157	8.0	0.00014	0.00630	1.46733 ± 15	3.79
Z-10	0.28165 ± 1	0.28165	2.2	0.28165	8.3	0.00012	0.00649	1.46739 ± 14	3.95
Z-11	0.28161 ± 2	0.28161	2.2	0.28160	8.1	0.00017	0.00817	1.46727 ± 13	3.59
Z-12	0.28162 ± 2	0.28162	2.2	0.28162	8.2	0.00011	0.00582	1.46728 ± 17	4.29
Z-13	0.28161 ± 2	0.28161	2.2	0.28161	8.2	0.00009	0.00498	1.46736 ± 10	4.14
Z-14	0.28158 ± 2	0.28158	2.2	0.28158	8.0	0.00009	0.00459	1.46735 ± 11	3.64
Z-15	0.28157 ± 1	0.28157	2.3	0.28157	8.0	0.00009	0.00509	1.46766 ± 10	3.72
Z-16	0.28162 ± 2	0.28162	2.2	0.28162	8.2	0.00013	0.00679	1.46710 ± 12	4.10
Z-17	0.28160 ± 2	0.28160	2.2	0.28160	8.1	0.00009	0.00472	1.46751 ± 15	4.08
Z-18	0.28160 ± 2	0.28160	2.2	0.28160	8.1	0.00007	0.00359	1.46745 ± 17	4.71
Z-19	0.28154 ± 2	0.28154	2.3	0.28154	7.9	0.00007	0.00365	1.46754 ± 14	4.15
Z-20	0.28156 ± 2	0.28156	2.3	0.28155	7.9	0.00012	0.00627	1.46760 ± 14	4.25
Z-21	0.28163 ± 2	0.28163	2.2	0.28163	8.3	0.00010	0.00528	1.46718 ± 17	4.23
Z-22	0.28169 ± 1	0.28169	2.1	0.28169	8.5	0.00004	0.00211	1.46722 ± 18	5.96
Z-23	0.28157 ± 1	0.28157	2.3	0.28157	8.0	0.00010	0.00516	1.46764 ± 17	3.94
Z-24	0.28158 ± 2	0.28158	2.3	0.28157	8.0	0.00010	0.00519	1.46689 ± 16	4.01
Z-25	0.28163 ± 2	0.28163	2.2	0.28162	8.2	0.00007	0.00343	1.46736 ± 15	3.79
Z-26	0.28155 ± 2	0.28155	2.3	0.28155	7.9	0.00013	0.00641	1.46744 ± 14	3.75
Z-27	0.28159 ± 2	0.28158	2.2	0.28158	8.0	0.00015	0.00778	1.46738 ± 16	4.11
Z–28	0.28163 ± 2	0.28163	2.2	0.28162	8.2	0.00015	0.00734	1.46735 ± 11	3.42
Whole rock eclogite									
MX8A	0.281822 ± 6	0.281804	2.2	0.281595	7.9	0.0054		1.46734 ± 2	4.12

T_{DM}: depleted mantle Hf model age. Initial Hf isotopic ratios were calculated using the depleted mantle model age and a decay constant $\lambda = 1.867 \times 10^{-11}$ yr^{-1} [59]. All errors are 1 sigma uncertainties.

mental diffusion data indicating that the Hf isotope system in zircon was essentially unperturbed whereas the U–Pb system was partially reset.

5.2. HFSE enrichment and zircon formation

Textural relationships document that garnet, clinopyroxene and zircon coexist in the Jericho eclogites, and provide evidence indicating that zircon is a constituent of the original eclogite mineral assemblage (Fig. 2). The incorporation of older zircon cores (i.e. xenocrystic origin) during eclogite metamorphism can be excluded based on their uniform Hf isotope composition. The unusual enrichment in Zr, Hf and other HFSE of the Jericho eclogites (enrichment of up to ~100 times; [14]) is not an inherent feature of mafic oceanic volcanics, which most probably were the precursor rocks to the Jericho eclogites. The excess HFSE could have been introduced just prior to or during eclogite formation as the result of interaction with CO_2-rich metasomatic melts [14], or, more likely, subduction-related fluids. HFSE enrichment and zircon formation as the result of fluid circulation in subduction zones have been demonstrated in studies on orogenic eclogites (e.g. [45,46]). These investigations indicate that high temperature subduction-related fluids (~600 °C, 20 kb) can transport HFSE that most probably have been dissolved in surrounding eclogite over short distances and concentrate these elements into a fluid phase. Similar studies on orogenic eclogite have proposed that high temperature, HFSE-enriched fluids generated in subduction shear zones between the mantle wedge and subducted oceanic crust may also play an important role as metasomatic agents in subduction zones (e.g. [47]). Crustal material may also have contributed to the excess HFSE observed in the Jericho eclogites. For example, continental sediments of Archean age in the Slave Province are characterized by a

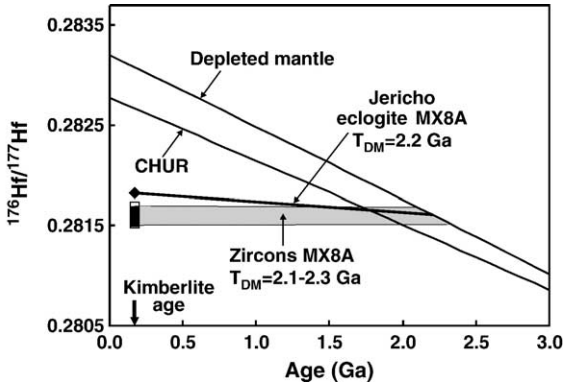

Fig. 6. Hf isotope evolution diagram for Jericho zircons (open boxes) and whole rock eclogite MX8A (filled diamond) showing depleted mantle model ages (T_{DM}). Evolution lines for a chondritic reservoir (CHUR) and depleted mantle [36,58] are also shown; 2σ errors smaller than symbol size.

relatively unradiogenic Hf isotopic composition (^{176}Hf/^{177}Hf values of ~0.2804 and ~0.2812 at 3.8 Ga and 2.5 Ga, respectively; e.g. [37,48]). Thus, incorporation of small amounts of continental sediments would alter (to some extent) the primary Hf isotope composition of the subducted oceanic crust.

5.3. Tectonic evolution of the Slave craton

Geophysical studies have demonstrated the existence of several seismic reflectors in the mantle beneath the Slave craton, strongly suggesting the presence of paleo-subduction surfaces in the subcontinental lithosphere [49,50]. These seismic profiles of the Slave lithosphere are entirely consistent with previous interpretations that the Jericho eclogites represent remnants of subducted and metamorphosed oceanic crust based on geochemical considerations [14,28]. At least two Precambrian subduction events have been well documented for the Slave craton, one at 2.7 to 2.6 Ga that led to the amalgamation of the Archean Slave craton; the other at its western margin occurring prior to ~1.9 Ga (e.g. [23,51]). Plate tectonic reconstruction models for the Slave Province indicate the existence of an oceanic basin between the Archean Anton (microcontinent, west direction) and the Contwoyto terranes (magmatic arc, east direction) in the late Archean, prior to the assembly of the Slave craton (e.g. [23,52]). The subduction of this Archean oceanic crust and subsequent terrane collision resulted in the amalgamation of the Slave craton ~2.6 Ga ago. Paleoproterozoic subduction processes and subsequent tectonic accretion of the 1.95–1.91 Ga Hottah terrane (continental magmatic arc) to the Slave craton during the Wopmay orogeny have also been well documented (e.g. [26]). Previous investigations focusing on the Jericho eclogites have proposed that their origin is linked to east-dipping subduction of oceanic mafic volcanics at the western margin of the Slave craton. This is evidenced by the Great Bear magmatic arc that developed at ~1.9 Ga after the collision of the Hottah terrane and the Slave craton [14,26,28]. This petrogenetic model has been proposed based on a synthesis of eclogite mineral compositions, the occurrence of calc-alkaline volcanism, and the results from seismic studies, while previous U–Pb dates postdate the event [14,26,28,49,50]. Alternatively, the formation of the Jericho eclogites may have been associated with subduction occurring at or prior to 1.95–1.91 Ga, generating the Hottah magmatic arc at the western margin of the Slave craton. Most importantly, the in-situ U–Pb date of 1989 ± 67 obtained for one Jericho zircon presented here is in good agreement with a tectonic model linking rock formation to Paleoproterozoic subduction, suggesting that eclogite formation occurred several tens of million years prior to calc-alkaline volcanism of the Hottah or Great Bear arcs. This appears plausible since it is most likely that generation of oceanic crust and its subsequent subduction predates the arc magmatism. The youngest Hf

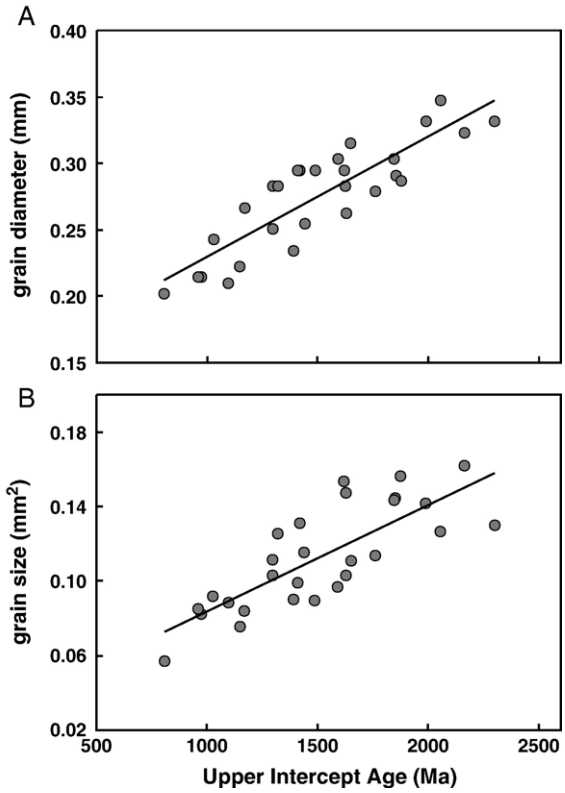

Fig. 7. Upper intercept age (Ma) versus (A) smallest grain diameter (mm) and (B) grain size (mm^2) for individual zircon analyses.

depleted mantle model ages (2.1 ± 0.1 Ga) for the Jericho zircons are slightly older than the U–Pb date of 1989 ± 67. This difference in age is to some extent expected since the Hf depleted mantle model ages reflect the oceanic crust formational age while the U–Pb date captures the timing of subsequent oceanic crust transformation into eclogite. Whereas the Hf model ages trend to somewhat older than those postulated for the Hottah or Great Bear magmatic events, these are nonetheless significantly younger than a 2.7 Ga subduction event. Thus, the 2.1 to 2.3 Ga old Hf model zircon ages may be interpreted to document a tectonic event not evidenced by other chronometers/isotope systems, or seismic and structural studies; alternatively, these represent intermediate ages produced via the binary mixing of Hf from at least two end member compositions.

One possible interpretation is that 'radiogenic' Hf originating from 2.1–2.0 Ga oceanic crust mixed with 'unradiogenic' Hf contained within the associated, overlying sediments during the subduction at the western margin of the Slave craton. The mixing of sediments into subducted oceanic crust has previously been documented and well-established (e.g. Lesser Antilles) and evidence for sediment input within arc volcanism has also been reported [53,54]. This sedimentary component could likely represent eroded Archean continental material emanating from the Slave Province, which is characterized by a relatively unradiogenic Hf isotopic composition (^{176}Hf/^{177}Hf values of ~0.2804 and ~0.2812 at 3.8 Ga and 2.5 Ga, respectively; e.g. [37,48]). This mixed Hf (originating from oceanic crust and sedimentary component) was scavenged into zircon via metasomatic fluids during the transformation of the oceanic crust to eclogite. The result is zircon yielding an intermediate Hf isotopic composition resulting in 'fictitiously' older Hf depleted mantle model ages up to 2.3 Ga (Fig. 8). The involvement of a small amount of Archean sediment in the formation of the Jericho zircons remains a plausible explanation for the slightly older Hf model ages since the Slave craton constitutes an evident source region for such material. An alternative interpretation for the Hf model ages of the Jericho zircons also involves binary mixing of Hf from two distinct sources; one involving Hf found within the transformed oceanic crust subducted at 2.7 to 2.6 Ga, and the other associated with the mantle plume giving rise to the pervasive Malley and Mackay dikes swarms at 2.23 and 2.21 Ga, respectively, within the Slave Province ([41]; Fig. 8). However, such a model would necessitate the scavenging of all the radiogenic Hf found within the precursor eclogite (within garnet and clinopyroxene), and its subsequent homogenization with Hf-bearing metasomatic fluids derived from the impinging mantle plume. This interpretation is less tenable given the significant difference that would have existed in the Hf isotope compositions between the original clinopyroxene and garnet; this would have reduced the likelihood of producing the relatively uniform Hf isotope ratios for the Jericho zircons. Thus, our preferred model invokes the incorporation of Hf found within the associated sediments into the 2.0 to 2.1 Ga old oceanic crust that was subducted at the western margin of the Slave craton.

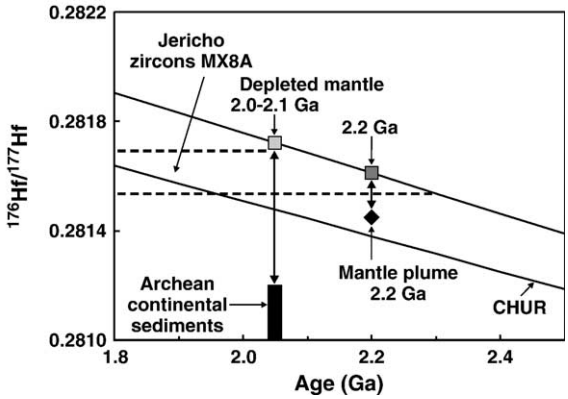

Fig. 8. Hf isotope evolution diagram for Jericho zircons (dashed field) showing possible mixing of oceanic crust (depleted mantle) with Archean sediments or mantle plume material (for further explanation see text).

The initial ^{176}Hf/^{177}Hf isotope compositions for the Jericho zircons listed in Table 2 correspond to positive ε_{Hf} values that range between +7.8 and +8.5. These positive ε_{Hf} values reported here contrast sharply to the negative ε_{Hf} values documented for both Groups I and II kimberlites from South Africa [55]. The source region giving rise to the Group I kimberlites is believed to originate from beneath the lithosphere, and derived from ancient, deeply subducted oceanic basalt that later became incorporated into the convecting mantle source [55]. A similar, ancient (>3.0 Ga old) unradiogenic mantle component is believed to have been the source region for other alkalic rock types, such as the carbonatite occurrences in Greenland [56]. Thus, the contrasting Hf isotopic nature of the Jericho zircons precludes derivation, or an origin from a similar deep, unradiogenic mantle reservoir that was sampled by the South African kimberlites. In addition, the involvement of Archean subcontinental lithospheric mantle can also be excluded as a source region for the Jericho zircons. The former is most likely characterized by much higher ε_{Hf} values (≥ +20) based on the Hf isotope compositions of low-temperature peridotites within the Nikos kimberlite pipe on Somerset Island, Canada [12]. Thus,

this lends further support to our model that the Jericho zircons were derived from a juvenile mantle component, such as subducted Paleoproterozoic oceanic crust. The time span between oceanic crust formation and its subsequent subduction cannot be exactly ascertained based on the Hf isotope data, but was most probably short-lived (i.e.<<100 million years).

6. Conclusions

This laser ablation zircon study demonstrates the robust nature of the Hf isotope system in zircon separated from a kimberlite-hosted mantle xenolith, and its resistance to isotope exchange in the lithosphere to temperatures of at least 1000 °C. This finding is in good agreement with previous studies that have demonstrated the capacity of the Lu–Hf chronometer in preserving the geological history of mantle xenoliths (and constituent garnets) that last equilibrated at subcontinental lithospheric conditions [12,57]. In contrast, U–Pb zircon dates record a complex geological history and can only provide minimum age constraints for mantle-derived rocks such as the Jericho eclogites.

Plate tectonic reconstruction models for the Slave Province propose the existence of east-dipping subduction regimes in the Paleoproterozoic. The Hf isotopic data reported here are consistent with the formation of the Jericho eclogites during the Proterozoic subduction of oceanic crust and subsequent production of subduction zone magmas that formed the Hottah or Great Bear magmatic arcs. The oldest Hf depleted mantle model ages (up to 2.3 Ga) most likely represent intermediate compositions resulting from the incorporation of 'crustal' Hf derived from associated sediments into the 2.1 to 2.0 Ga ocean crust during its subduction, and subsequent transformation into eclogite at ~2 Ga beneath the Slave craton.

Acknowledgments

Funding for this study was provided by Alberta Ingenuity Fund through a postdoctoral fellowship to S. Schmidberger. The Radiogenic Isotope Facility at the University of Alberta is supported by a NSERC Major Facilities Access Grant. We thank two anonymous reviewers for their thorough comments that greatly improved the manuscript.

References

[1] D.G. Pearson, The age of continental roots, Lithos 48 (1999) 171–194.

[2] D.E. Jacob, Nature and origin of eclogite xenoliths from kimberlites, Lithos 77 (2004) 295–316.

[3] P. Deines, J.W. Harris, J.J. Gurney, Carbon isotope ratios, nitrogen content and aggregation state, and inclusion chemistry of diamonds from Jwaneng, Botswana, Geochim. Cosmochim. Acta 61 (1997) 3993–4005.

[4] R.M. Davies, W.L. Griffin, N.J. Pearson, A.S. Andrew, B.J. Doyle, S.Y. O'Reilly, Diamonds from the deep; Pipe DO-27, Slave Craton, Canada, 7th International Kimberlite Conference Proc., 1999, pp. 148–155.

[5] M.J. O'Hara, H.S. Yoder, Formation and fractionation of basic magmas at high pressure, Scott. J. Geol. 3 (1967) 67–117.

[6] H. Helmstaedt, R. Doig, Eclogite nodules from kimberlite pipes of the Colorado plateau – samples of subducted Franciscan-type oceanic lithosphere, Phys. Chem. Earth 9 (1975) 95–111.

[7] M. Barth, R.L. Rudnick, I. Horn, W.F. McDonough, M.J. Spicuzza, J.W. Valley, S.E. Haggerty, Geochemistry of xenolithic eclogites from West Africa: Part 2. Origins of the high MgO eclogites, Geochim. Cosmochim. Acta 66 (2002) 4325–4345.

[8] D.G. Pearson, S.B. Shirey, R.W. Carlson, F.R. Boyd, N.P. Pokhilenko, N. Shimizu, Re–Os, Sm–Nd, and Rb–Sr isotope evidence for thick Archean lithospheric mantle beneath the Siberian craton modified by multistage metasomatism, Geochim. Cosmochim. Acta 59 (1995) 959–977.

[9] S.S. Schmidberger, A. Simonetti, D. Francis, Sr–Nd–Pb isotope systematics of mantle xenoliths from Somerset island kimberlites: evidence for lithosphere stratification beneath Arctic Canada, Geochim. Cosmochim. Acta 65 (2001) 4243–4255.

[10] A.J. Erlank, F.G. Waters, C.J. Hawkesworth, S.E. Haggerty, H.L. Allsopp, R.S. Rickard, M.A. Menzies, Evidence for mantle metasomatism in peridotite nodules from the Kimberley pipes, South Africa, in: M.A. Menzies, C.J. Hawkesworth (Eds.), Mantle Metasomatism, Academic Press, London, 1987, pp. 221–311.

[11] M.A. Menzies, Archean, proterozoic, and phanerozoic lithospheres, in: M.A. Menzies (Ed.), Continental Mantle, Oxford University Press, Oxford, 1990, pp. 67–86.

[12] S.S. Schmidberger, A. Simonetti, D. Francis, C. Gariépy, Probing Archean lithosphere using the Lu–Hf isotope systematics of Peridotite Xenoliths from Somerset Island Kimberlites, Canada, Earth Planet. Sci. Lett. 197 (2002) 245–259.

[13] Y.D. Chen, S.Y. O'Reilly, P.D. Kinny, W.L. Griffin, Dating lower crust and upper mantle events: an ion microprobe study of xenoliths from kimberlitic pipes South Australia, Lithos 32 (1994) 77–94.

[14] L.M. Heaman, R.A. Creaser, H.O. Cookenboo, Extreme enrichment of high field strength elements in Jericho eclogite xenoliths: a cryptic record of Paleoproterozoic subduction, partial melting, and metasomatism beneath the Slave craton, Canada, Geology 30 (2002) 507–510.

[15] U. Schärer, F. Corfu, D. Demaiffe, U–Pb and Lu–Hf isotopes in baddeleyite and zircon megacrysts from the Mbuji–Mayi kimberlite: constraints on the subcontinental mantle, Chem. Geol. 143 (1997) 1–16.

[16] P.D. Kinny, W. Compston, J.W. Bristow, I.S. Williams, Archean mantle xenocrysts in a Permian kimberlite: Two generations of kimberlit ic zircon in Jwaneng DK2, southern Botswana, Geol. Soc. Aust. Spec. Publ. 14 (1989) 833–842.

[17] W.L. Griffin, N.J. Pearson, E. Belousova, S.E. Jackson, E. van Achterbergh, S.Y. O'Reilly, S.R. Shee, The Hf isotope composition of cratonic mantle: LAM-MC-ICPMS analysis of zircon megacrysts in kimberlites, Geochim. Cosmochim. Acta 64 (2000) 133–147.

[18] J.A. Baldwin, S.A. Bowring, M.L. Williams, I.S. Williams, Eclogites of the Snowbird tectonic zone: petrological and U–Pb geochronological evidence for Paleoproterozoic high-pressure metamorphism in the western Canadian Shield, Contrib. Mineral. Petrol. 147 (2004) 528–548.
[19] A.S. Collins, S.M. Reddy, C. Buchan, A. Mruma, Temporal constraints on paleoproterozoic eclogite formation and exhumation (Usagaran Orogen, Tanzania), Earth Planet. Sci. Lett. 224 (2004) 175–192.
[20] D.J. Cherniak, J.M. Hanchar, E.B. Watson, Diffusion of tetravalent cations in zircon, Contrib. Mineral. Petrol. 127 (1997) 383–390.
[21] S.A. Bowring, I.S. Williams, Priscoan (4.00–4.03 Ga) orthogneisses from northwestern Canada, Contrib. Mineral. Petrol. 134 (1999) 3–16.
[22] W.J. Davis, W. Bleeker, Timing of plutonism, deformation, and metamorphism in the Yellowknife Domain Slave Province, Canada, Can. J. Earth Sci. 36 (1999) 1169–1187.
[23] P.F. Hoffman, Precambrian geology and tectonic history of North America, in: A.W. Bally, A.R. Palmer (Eds.), The Geology of North America–An overview, Geol. Soc. America, Boulder, Colorado, 1989, pp. 447–512.
[24] J.A. Pell, Kimberlites in the Slave craton Northwest Territories, Canada, Geosci. Can. 24 (1997) 77–91.
[25] S.E. Price, J.K. Russell, M.G. Kopylova, Primitive magma from the Jericho pipe, N.W.T., Canada: constraints on primary kimberlite melt chemistry, J. Petrol. 41 (2000) 789–808.
[26] R.S. Hildebrand, P.F. Hoffman, S. Bowring, Tectono-magmatic evolution of the 1.9 Ga Great Bear magmatic zone, Wopmay orogen, northwestern Canada, J. Volcanol. Geotherm. Res. 32 (1987) 99–118.
[27] M.G. Kopylova, J.K. Russell, H. Cookenboo, Upper-mantle stratigraphy of the Slave craton, Canada: insights into a new kimberlite province, Geology 26 (1998) 315–318.
[28] M.G. Kopylova, J.K. Russell, N.I. Christensen, Composition and fabric of the Northern Slave eclogite as evidence for mantle metasomatism, Lithoprobe Report, vol. 81, 2001, pp. 61–70.
[29] E.J. Krogh, The garnet-clinopyroxene Fe–Mg geothermometer – a reinterpretation of existing experimental data, Contrib. Mineral. Petrol. 99 (1988) 44–48.
[30] A. Simonetti, L.M. Heaman, R.P. Hartlaub, R.A. Creaser, T.G. MacHattie, C. Böhm, U–Pb zircon dating by laser ablation-MC-ICP-MS using a new multiple ion counting Faraday collector array, J. Anal. At. Spectrom. 20 (2005) 677–686.
[31] R.N. Taylor, T. Warneke, J.A. Milton, I.W. Croudace, P.E. Warwick, R.W. Nesbitt, Multiple ion counting determination of plutonium isotope ratios using multi-collector ICP-MS, J. Anal. At. Spectrom. 18 (2003) 480–484.
[32] L.P. Black, B.L. Gulson, The age of the Mud Tank carbonatite, Strangways Range Northern Territory, BMR, J. Aust. Geol. Geophys. 3 (1978) 227–232.
[33] N. Machado, A. Simonetti, U–Pb dating and Hf isotopic composition of zircon by laser ablation-MC-ICP-MS, Laser Ablation-ICPMS in the Earth Sciences, Mineral. Ass. Canada Short Course, vol. 29, 2001, pp. 121–146.
[34] J. Woodhead, J. Hergt, M. Shelley, S. Eggins, R. Kemp, Zircon Hf-isotope analysis with an excimer laser, depth profiling, ablation of complex geometries, and concomitant age estimation, Chem. Geol. 209 (2004) 121–135.
[35] M. Bizzarro, J.A. Baker, D. Ulfbeck, A new digestion and chemical separation technique for rapid and highly reproducible determination of Lu/Hf and Hf isotope ratios in geological materials by MC-ICP-MS, Geostand. Newsl. 27 (2003) 133–145.
[36] J.D. Vervoort, P.J. Patchett, J. Blichert-Toft, F. Albarède, Relationships between Lu–Hf and Sm–Nd isotopic systems in the global sedimentary system, Earth Planet. Sci. Lett. 168 (1999) 79–99.
[37] Y. Amelin, D.-C. Lee, A.N. Halliday, Early–middle Archean crustal evolution deduced from Lu–Hf and U–Pb isotopic studies of single zircon grains, Geochim. Cosmochim. Acta 64 (2000) 4205–4225.
[38] J.K.W. Lee, I.S. Williams, D.J. Ellis, Pb, U and Th diffusion in natural zircon, Nature 390 (1997) 159–162.
[39] G.R. Tilton, Volume diffusion as a mechanism for discordant lead ages, J. Geophys. Res. 65 (1960) 2933–2945.
[40] G.J. Wasserburg, Diffusion processes in lead–uranium systems, J. Geophys. Res. 68 (1963) 4823–4846.
[41] A.N. LeCheminant, L.M. Heaman, O. van Breemen, R.E. Ernst, W.R.A. Baragar, K.L. Buchan, Mafic magmatism, mantle roots, and kimberlites in the Slave craton, in: A.N. LeCheminant, D.G. Richardson, R.N.W. DiLabio, K.A. Richardson (Eds.), Searching for Diamonds, Geol. Survey Canada Open File 3228, 1996, pp. 161–169.
[42] A.N. LeCheminant, L.M. Heaman, Mackenzie igneous events, Canada: Middle Proterozoic hotspot magmatism associated with ocean spreading, Earth Planet. Sci. Lett. 96 (1989) 38–48.
[43] S.S. Harlan, L.M. Heaman, A.N. LeCheminant, W.R. Premo, Gunbarrel mafic magmatic event: a key 780 Ma time marker for Rodinia plate reconstructions, Geology 31 (2003) 1053–1056.
[44] L.M. Heaman, A.N. LeCheminant, R.H. Rainbird, Nature and timing of Franklin igneous events, Canada: implications for a late Proterozoic mantle plume and the break-up of Laurentia, Earth Planet. Sci. Lett. 109 (1992) 117–131.
[45] S. Nadeau, P. Philippot, F. Pineau, Fluid inclusion and mineral isotopic compositions (H–O–C) in eclogitic rocks as tracers of local fluid migration during high-pressure metamorphism, Earth Planet. Sci. Lett. 114 (1993) 431–448.
[46] D. Rubatto, J. Hermann, Zircon formation during fluid circulation in eclogites (Monviso, Western Alps): implications for Zr and Hf budget in subduction zones, Geochim. Cosmochim. Acta 67 (2003) 2173–2187.
[47] S.S. Sorensen, J.N. Grossman, Enrichment of trace elements in garnet amphibolites from a paleo-subduction zone: Catalina Schist, southern California, Geochim. Cosmochim. Acta 53 (1989) 3155–3177.
[48] R.K. Stevenson, P.J. Patchett, Implications for the evolution of continental crust from Hf isotope systematics of Archean detrital zircons, Geochim. Cosmochim. Acta 54 (1990) 1683–1697.
[49] M.G. Bostock, Anisotropic upper-mantle stratigraphy and architecture of the Slave craton, Nature 390 (1997) 392–395.
[50] F.A. Cook, A.J. van der Velden, K.W. Hall, Frozen subduction in Canada's Northwest Territories: lithoprobe deep lithospheric reflection profiling of the western Canadian Shield, Tectonics 18 (1999) 1–24.
[51] W. Bleeker, The late Archean record: a puzzle in ca. 35 pieces, Lithos 71 (2003) 99–134.
[52] W.K. Fyson, H. Helmstaedt, Structural patterns and tectonic evolution of supracrustal domains in the Archean Slave Province, Canada, Can. J. Earth Sci. 25 (1988) 301–315.
[53] J.P. Davidson, Isotopic and trace element constraints on the petrogenesis of subduction related lavas from Martinique, Lesser Antilles, J. Geophys. Res. 91 (1986) 5943–5962.

[54] W.M. White, B. Dupré, Sediment subduction and magma genesis in the Lesser Antilles: isotopic and trace element constraints, J. Geophys. Res. 91 (1986) 5927–5941.
[55] G.M. Nowell, D.G. Pearson, D.R. Bell, R.W. Carlson, C.B. Smith, P.D. Kempton, S.R. Noble, Hf isotope systematics of kimberlites and their megacrysts: new constraints on their source regions, J. Petrol. 45 (2004) 1583–1612.
[56] M. Bizzarro, A. Simonetti, R.K. Stevenson, J. David, Hf isotope evidence for a hidden mantle reservoir, Geology 30 (2002) 771–774.
[57] R.-M. Bedini, J. Blichert-Toft, F. Albarède, Isotopic constraints on the cooling of the continental lithosphere, Earth Planet. Sci. Lett. 223 (2004) 99–111.
[58] J. Blichert-Toft, F. Albarède, The Lu–Hf isotope geochemistry of chondrites and the evolution of the mantle-crust system, Earth Planet. Sci. Lett. 148 (1997) 243–258.
[59] E. Scherer, C. Münker, K. Mezger, Calibration of the lutetium–hafnium clock, Science 293 (2001) 683–687.